Experimental validation of simulation methods for bi-directional transmission properties at the daylighting performance level

A Report of
IEA SHC TASK 31 / IEA ECBCS ANNEX 29: Daylighting Buildings in the 21st Century
April 2005

Disclaimer

This report was printed and is available at:

Institute and adress

Price: xx,- Eur T31/C-xx/GER/04-6

Experimental validation of simulation methods for bi-directional transmission properties at the daylighting performance level

International Energy Agency (IEA)
Solar Heating and Cooling Programme Task 31

DAYLIGHTING BUILDINGS IN THE 21ST CENTURYDAYLIGHT

Edited by Fawaz MAAMARI
ENTPE
Rue Maurice Audin
69518 Vaulx en Velin Cedex - France

DISTRIBUTION CLASSIFICATION: UNRESTRICTED

PREFACE

The main objectives of the IEA Solar Heating and Cooling Programme (SHC) Task 31 "Daylighting Buildings in the 21st Century" is to advance daylighting technologies and to promote daylight conscious building design. Task 31 continues until August 2005, and will endeavour to overcome the barriers that are impending the appropriate integration of daylighting aspects in building design. The participants in this task are Australia, Belgium, Canada, Denmark, Finland, France, Germany, Italy, Japan, Netherlands, New Zealand, Norway, Sweden, Switzerland, United Kingdom and the United States. Australia is the Operating Agent.

The objective of this Subtask C "Daylighting Design Tools" of Task 31 is to improve the knowledge and quality of lighting tools to enable building designers to predict the energy performance and visual comfort conditions of complex fenestration systems in their daily working process. This Subtask will make a link between industry, designers and software developers and promote the tools to the practitioners. The research work in this subtask concentrated on four topics:

C1: User Interfaces
C2: Algorithms and Plugins
C3: Promotion of Tools and Engines
C4: Validation

Acknowledgements

This report is the result of collaboration between the following participants:
Fawaz Maamari, Marilyne Andersen, Jan de Boer, William L. Carroll, Dominique Dumortier, Phillip Greenup.

- Fawaz Maamari was supported by the National School of the State Public Works (ENTPE).
- Jan de Boer was supported by the German Ministry of Economics and Labour (BMWA) under grant nr. 0329037G and by the ADELINE User Club.
- Marilyne Andersen was supported by the Swiss Federal Institute of Technology (EPFL) and the Commission for Technology and Innovation (CTI) during her PhD thesis, as well as by a joint funding from the Lawrence Berkeley National Laboratory and the Swiss National Science Foundation, fellowship 81EL-66225, during her stay at LBNL. She is supported by the Massachusetts Institute of Technology since July 2004. She would like to thank Lambda Research Corporation for having provided her with a license of TraceProTM to complete this research.
- William Carroll was supported at Lawrence Berkeley National Laboratory by the Assistant Secretary for Energy Efficiency and Renewable Energy, Office of Building Technology, Building Technologies Program, of the U.S. Department of Energy under Contract No. DE-AC03-76SF00098.

EXECUTIVE SUMMARY

The objective of this report is to assess the capability of existing lighting simulation methods to predict the performance of complex fenestration systems, which are becoming a commonly used component in buildings construction domain.

A specific experimental protocol was conducted to collect reliable reference data (with a minimum of error sources and uncertainty margins) based on illuminance measurements inside a black box with (and without) one complex glazing sample facing a measured external luminance distribution. Two different samples were used: a SerraglazeTM element and a Laser Cut Panel.

Two types of simulation methods were tested and compared: The first is based on modeling the glazing sample in a ray-tracing simulation program and the second is based on use of the samples' BTDF data, which was produced by means of three different assessment methods (one measurement and two simulations). The various BTDF data sets were combined with the external luminance distribution to predict the flux distribution inside the room and the resulting illuminance values at the reference points.

The comparison between the experimental reference data and the simulation results showed that the influence of the CFS could be predicted with a reasonable accuracy. The simplicity of the testing scenarii allowed to highlight the weakness areas of the applied simulation methods and the influence of the accuracy in the physical description of the samples. Finally, some recommendations were made for a better use of the existing simulation methods.

CONTENTS

1. INTRODUCTION

Since the early nineties, Complex Fenestration Systems (CFS) made their way to the buildings of the 21st century [1, 2, 3]. The first objective of using CFSs is to optimize the availability and uniformity of daylighting inside buildings and to contribute to reducing energy consumption for artificial light during daytime.

Predicting the performance of such systems is one of the main difficulties facing the lighting simulation domain, despite the remarkable progress observed in this field for the last two decades [2, 4, 5, 6, 7, 8].

To improve the performances of daylighting simulation programs and achieve reliable modeling of light propagation in rooms using CFS, the spatial distribution of daylight must be characterized precisely, in a similar way as for lighting fixtures [9, 10, 11]. This is done by assessing the Bidirectional Transmission (or Reflection) Distribution Function (BTDF, BRDF) of such materials, defined by the Commission Internationale de l'Eclairage [12] as the "quotient of the luminance of the medium by the illuminance on the medium".

Many efforts are being investigated internationally to propose new experimental methods for assessing the Bi-directional Transmission Distribution Function (BTDF) of CFS [2, 13, 14, 15, 16, 17] as well as alternative approaches based on ray-tracing simulations [18, 19, 20, 21]. The extent to which such simulation methods are accurate is, however, difficult to verify, and predicting the performances of CFS in buildings hence appears as a critical issue. This difficulty is mainly related to the lack of reliable validation data and to the usually high uncertainties in existing experimental reference data [22, 23, 24, 25].

Within this context, this paper proposes and applies a validation approach for assessing the capability and accuracy of existing methods in predicting the performance of a CFS with regard to the illuminance distribution inside a room. These simulation methods can be based on the use of calculated or measured BTDF but can also be any other type of methods like ray-tracing based simulations. The proposed validation approach aims in particular at highlighting and minimizing the uncertainties in the experimental reference data [23]. The paper also highlights the other parameters (in addition to the description of the reference scenario) affecting the accuracy of a CFS simulation: the quality of the BTDF raw data and the algorithms used to calculate the light distribution from CFS or toward the different surfaces of a room.

The paper starts by describing the experimental set-up used to collect the reference data with an estimation of the related uncertainties (section 2), in section 3 a description of the BTDF assessment methods is given and the related error sources is discussed, in section 4 the different algorithms used to conduct CFS simulations are presented and related error sources estimated, and finally the results comparisons are presented in section 5.

2. EXPERIMENTAL SET-UP FOR REFERENCE DATA

To assess the influence of a CFS on the illuminance distribution inside a room, an experimental set-up including a scale model, and artificial sky, a calibrated CCD camera and different photosensors was set-up.

The illuminance variation inside the scale model was measured with and without a CFS sample over the opening surface. For each measurement point, the ratio determined the directional transmission of the sample in the direction of the measurement point due to the external hemispherical luminance distribution. This ratio is used as a reference value to which the results of the tested simulation methods will be compared; in this paper, it will be referred to as the hemi-directional transmission (HDT).

The use of the hemi-directional transmission as a reference value allows to minimize the error sources related to the accurate description of the scenario including the external luminance distribution and the scale model dimensions and photometry. However, an estimation of the remaining error sources is made to calculate a margin of uncertainties that is assigned to the reference values.

2.1 Scale model description

The scale model was developed and used at ENTPE [25]. It consisted of a wooden cubic box of dimensions of 80cm×80cm×60cm, representing a room of 4m×4m at a 1:5 scale. Different sizes of vertical or horizontal openings were allowed, but only a 20cm×20cm (3.6cm thick) roof opening was used for the purpose of this study (see Figure 1).

All interior surfaces were painted with a matt black with a reflectance of 4.5% +/- 1%. The bi-directional reflection aspect of the painted surfaces was measured with a plane goniophotometer and was found to closely fit the Lambertian model (see Figure 2).

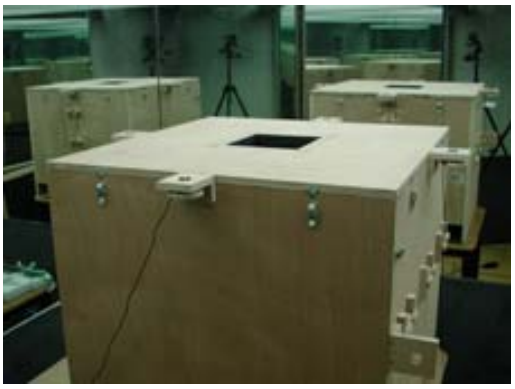

Figure 1. ENTPE scale model

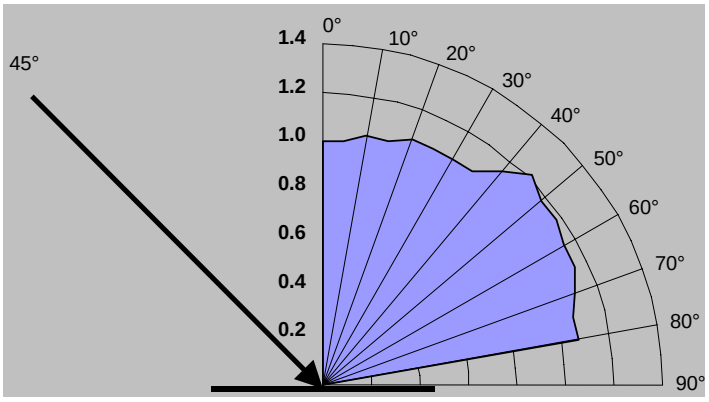

Figure 2. Example of the measured bi-directional reflection

Photocells were accurately positioned inside the scale model at vraious locations on the floor, wall surfaces as shown in Figure 3, and on the opening level for external illuminance measurements as shown in Figure 1.

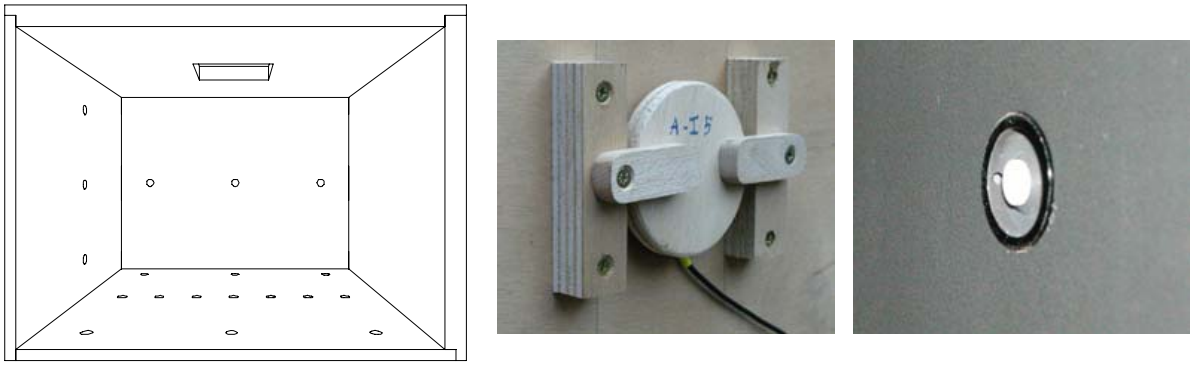

Figure 3. Measurement points locations and photocell positioning system

The positioning system provided by the scale model for a CCD camera with a Fisheye lens was used to measure the external luminance distribution as seen from the opening surface level (see Figure 4).

A complete description of the scale model can be found in [25].

Figure 4. Camera positioning systems for artificial and real sky scenarii

2.2 Luminance maps measurements

One of the main error sources when comparing daylighting simulations to experimental measurements is related to the description of the external luminance map, which is usually limited to an approximation or a simplification of the luminance distribution of an artificial or a real sky. This error source is particularly important in the case of a CFS where illuminance distribution is very sensitive to the directionality of the incoming light.

To minimize the related error sources, we measured the external luminance distribution simulteneously with the illuminance measurements inside and outside the scale model.

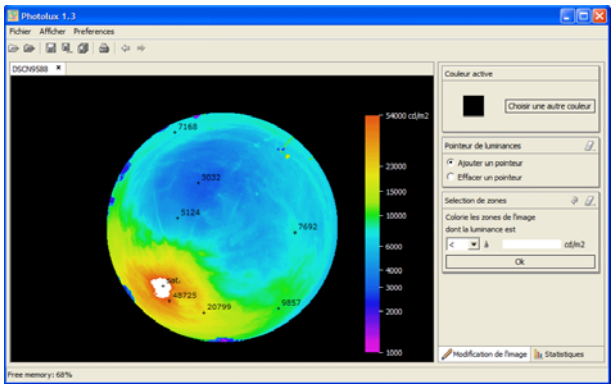

Figure 5. Using calibrated photos to produce a luminance map in Photolux

The luminances were measured by using the Photolux system developed at ENTPE [26], based on the use of a calibrated CCD camera (Nikon™ Coolpix model 990) equipped with a fish-eye lens and a dedicated software. The fish-eye lens allows an hemispherical luminance distribution to be covered.

The Photolux software produces a luminance map from one or more images (see Figure 5). Different photos (with different settings) may be needed to avoid saturated or under-exposed zones in the case of high range of luminance variation (from a few cd/m^2 to more than 10,000 cd/m^2). As the maximum luminance that can be measured with the Coolpix 990 is close to 50,000 cd/m^2, the system cannot provide information on the luminance of the sun and its circumsolar.

The produced luminance map is made of about 360,000 values and provides a quasi-continuous representation of the luminance of a scene. The luminance maps were saved in the Radiance sky format in 1° and 5° steps or into an equivalent intensity distribution file using the IESNA format.

The accuracy of the measured luminance values was close to 20%. To reduce this error further, a correction scale factor was introduced on the measured values accounting for the difference between the measured external illuminance and the value that was calculated from the measured luminance map.

The proposed procedure to describe and simulate the sky luminance map had been tested in [25] for empty openings, where a very good accuracy could be observed when the external illuminance corrections were included and the highly saturated zones avoided.

2.3 Scenarii and experimental protocols

Two different types of scenarii were tested, the first with a Serraglaze™ sample under an artificial sky, the second with an LCP sample under external real sky.

The main differences between the protocols of the two scenarii are related to the stability of the luminance distribution and to the possibility of measuring luminance maps at the same time as illuminance measurements. The LCP Scenario presented a higher directionality in the sky luminance distribution, which allowed the bi-directional influence of the material to be highlighted better.

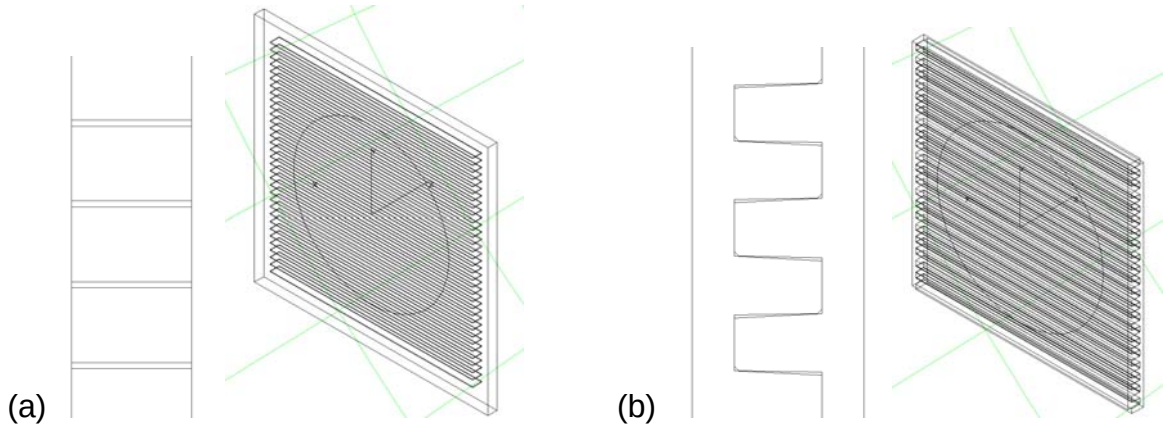

Figure 6. Illustration of the considered complex glazing materials. (a) Laser Cut Panel. (b) Serraglaze™.

2.3.1 Serraglaze™

The Serraglaze™ material is an optically variable device made of two identical crenellated plastic panels facing each other and shifted by half a period to fit into each other (see Figure 6(b)). The resulting thickness of the panel is 7 mm (2.27 mm for each exterior layer, 4.73 for the crenels), the crenels being cut at slightly off-horizontal slopes (3° when edge is full, 1° when edge is cut off at 45°, see Figure 6(b)). These specific geometric features were given by the manufacturer, and could not be experimentally verified on the available sample.

The Serraglaze™ scenarii were conducted inside the artificial sky of the ENTPE, which is a 2m×2m×2.1m room with four mirror walls and a luminous ceiling. The luminance distribution was close to a CIE overcast sky. The advantage of the artificial sky relies in the stability of the luminance distribution allowing minimal related error sources.

The scale model was positioned at the center of the artificial sky with the top level at about 145cm from the ground. Six measurement points were used inside the model as shown in Figure 7.

The Serraglaze™ sample was positioned at the top of the roof opening (see Figure 8), with the linear air gaps perpendicular to the measurement axis.

Measurements were taken for three scenarii with different luminance distributions (see Figure 9): Scenarii 2 and 3 were obtained by masking one of the mirror walls and by positioning the scale model at a different distance from the masked wall. For Scenarii 2 and 3, the sample edges were masked with a black tape (to avoid related error sources) leaving a 20cm square opening at the top level and an 18cm square opening at the bottom.

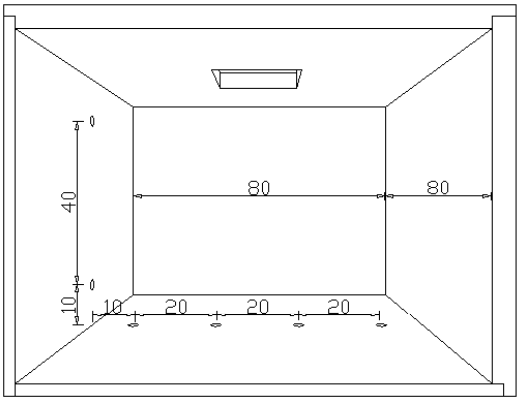

Figure 7. Measurement points positions for the Serraglaze™ scenarii

Figure 8. Scale model with the Serraglaze™ sample over the opening surface

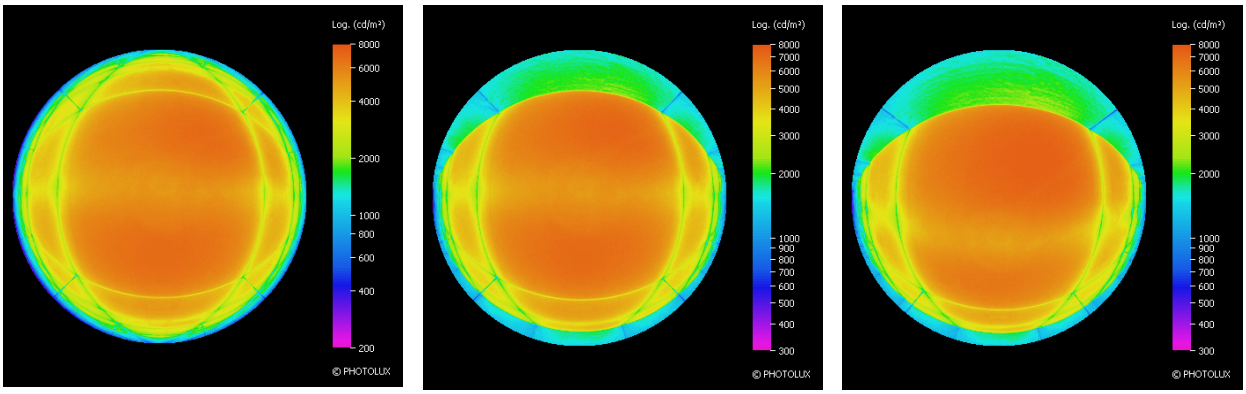

Figure 9. Luminace maps for scenarii 1, 2 and 3

The illuminance measurements were first taken with an empty opening then with the sample positioned at its center. The roof element was then removed and replaced by the camera positioning system to capture pictures of the artificial sky from the center of the opening, thus reducing error sources related to a near field situation [25, 27]. The external illuminance was measured simultaneously with both the image capture and internal measurements to verify the stability of the luminance distribution.

The measured values were corrected to account for the difference between measured external illuminance and the one calculated from the luminance map [25].

2.3.2 Laser Cut Panel

The Laser Cut Panel (LCP) is made of an acrylic panel of thickness 6 mm and dimensions 300 x 300 mm, through which a series of parallel cuts were made with a laser beam every 4 mm (the cuts themselves extend over 0.3 mm, see Figure 6(a)).

The LCP scenario was conducted on the roof of ENTPE with negligible surrounding masks and under an intermediate sky condition where the sun was hidden by clouds as shown in Figure 11. The main advantage of using real sky conditions lies in the optimal directionality of the luminance distribution, resulting in a more interesting illuminance variation inside the scale model for highlighting the influence of the LCP. Its disadvantage is

related to the variability of the luminance distribution, partly compensated by taking pictures and illuminance measurements simultaneously.

The sample was positioned at the top of the roof opening with the panel's cuts perpendicular to the measurement axis. The edges of the sample were not masked.

Nine measurement points were used inside the model (see Figure 10) in addition to the one for the external illuminance.

Illuminance measurements were first taken with an empty opening then with the sample positioned at the center of the opening. Pictures of the sky luminance distribution were taken simultaneously with each pair of measurements so that the difference between the calculated and the measured external illuminance could be determined. Based on this difference, a scaling ratio was applied to the luminance map.

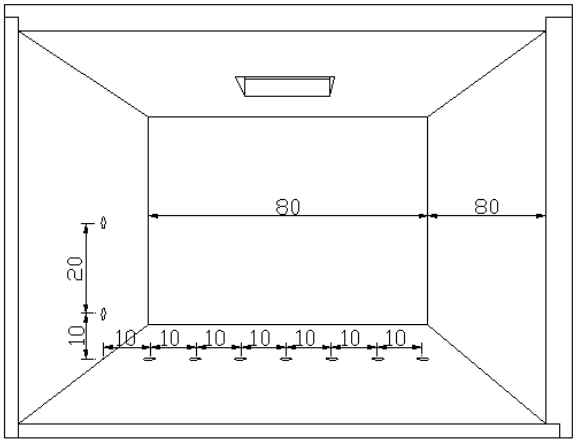

Figure 10. Measurement points positions

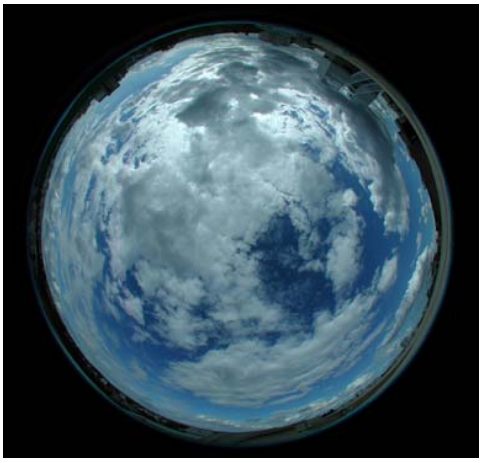

Figure 11. Sky condition during the LCP scenario

2.4 Estimation of the uncertainties in the reference data

The accuracy of a lighting simulation is first affected by the physical description of the scenario. Within a validation context, uncertainties due to inaccurate descriptions of the scenario and to the measurements themselves have to be taken into consideration for an objective comparison with the simulation results [23, 24].

These uncertainties should be estimated based on the identified error sources by using the following relation:

$U = \sqrt{\sum_i (Error_{(i)})^2}$ where i is the number of error sources.

The reference data can then be presented by mean of it's upper and lower tolerance limits (=measured value + or – the estimated uncertainties), within which simulation results should remain for acceptable accuracy (See Figure 12).

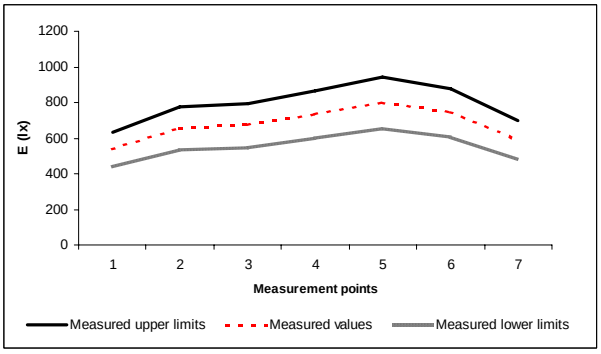

Figure 12. Presentation of the reference data by mean of upper and lower uncertainty limits

Nevertheless, it should be noted that some error sources are difficult to estimate.

This section presents the estimated uncertainties for the Serraglaze™ and LCP scenarii in addition to the list of identified error sources. The errors related to the BTDF data are not taken into consideration in the tolerance margins but are described separately in section 3.3.

2.4.1 Serraglaze™ scenarii

For an empty opening under the artificial sky, the measurements' uncertainty was estimated to +/- 10% taking into consideration the following error sources [25]: photocells calibration, photocells cosine correction, spectral sensibility, flux variation, photocells position, near field, surface reflectance (accuracy, homogeneity and directionality), geometry dimensions, and the external luminance distribution.

For the measurements with the Serraglaze™ sample, the error sources were similar to the empty opening in addition to an error source related to the positioning of the sample. The resulting uncertainty was estimated at 13%.

For the hemi-directional transmission, most of the error sources related to the scenario description were avoided or minimized with the exception of the luminance distribution and the positioning of the sample, leading to an uncertainty estimated at 10%.

It should be noted that for simplicity reasons the same uncertainty value was used for the 3 scenarii, and this is despite the difference related to the near filed error source, which is difficult to quantify [27].

The near field error source refers to the difference between the luminance field seen by a measurement point and the simulated one: the Figure 13 shows the example of the ENTPE scale model (with a 40cmx40cm opening) inside the ENTPE artificial sky. The angle of view between P4 and the opening allows defines the "real" zone of the sky seen by this point. This angle is used in the simulation to define the "Simulated" zone of the sky luminance map to be used for calculating the direct illuminance at P4: in our case, the sky luminance map is measured from the center of the opening. The difference between the luminance of the "Real" and the "Simulated" zones is equal to the error introduced to the simulation results. The Figure 14 shows the influence of this error on the correlation between measured and simulated values: when correcting the simulated illuminance values (by taking into consideration the calculated near field error source for each reference point), the correlation with the reference value is enhanced considerably [25].

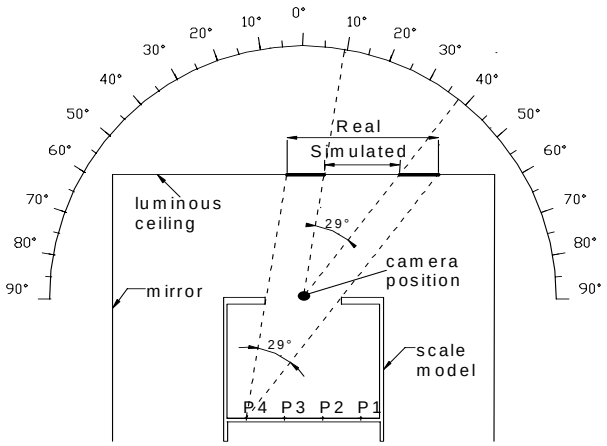

Figure 13. Illustration of the near field error source

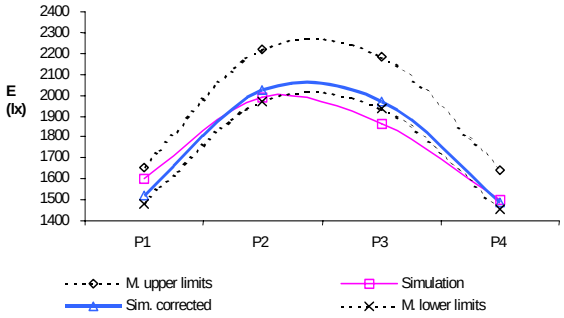

Figure 14. Influence of the near field corrections on the correlation between measurements and simulation results

For this study, the near field error source is less important due to the size of the opening, however it increases between scenario 1 and 3 where the scale model is closer to the artificial sky wall and where we have higher variations in the luminance distribution.

2.4.2 LCP scenario

The difference of this scenario with the previous one is related to the absence of the near field error source and mainly to the higher level of the error sources related to the luminance map and to the sample position (due to the high directionality in the luminance distribution).

The estimated uncertainty is 10% for the empty opening, 18% for the measurements with the LCP sample and 15% for the hemi-directional transmission.

3. ASSESSMENT OF BTDFS

Three of the four presented simulation methods in this paper are based on the use of BTDF data. The BTDF data of the tested samples were obtained by means of three different methods: one experimental approach based on digital imaging techniques, and two numerical methods based on ray-tracing techniques. A short description of these methods is given in this section while detailed information can be found in [28].

3.1 Bidirectional video-goniophotometer

The experimental assessment of BTDFs was achieved with an innovative bidirectional goniophotometer based on digital imaging techniques developed at LESO-PB / EPFL. Instead of being scanned by moving a sensor from point to point, the light flux emerging from the investigated sample is collected by a diffusing flat screen, at which a calibrated Charge-Coupled Device (CCD) camera is aiming, used as a multiple-points luminance-meter. To cover all possible emerging directions (2π steradian), the camera and the screen perform rotations of a 60° angle magnitude, leading to the visualization of the whole transmitted (reflected) hemisphere in a continuous way within a few minutes [17, 29].

This novel approach significantly reduces the time needed to monitor BT(R)DF data, lowering it down to a few minutes per incident direction instead of several hours for conventional assessment methods. This is a critical parameter in BT(R)DF assessment as about a hundred incident directions are usually required. At the same time, it allows the gathering of continuous transmitted (reflected) light distribution figures, only limited in resolution by the pixellisation of the digital images. The emerging hemisphere is indeed split into a regular grid of averaging sectors. Any risk of missing a discontinuity in the emerging luminance figure is thus prevented.

3.2 Numerical goniophotometers

LESO-PB / EPFL

The experimental conditions described above were reproduced virtually with the commercial forward ray-tracer TracePro®[1] based on Monte Carlo calculations [20,21]. The simulation model included a detection screen split into the same pattern of angular sectors as for the measurements and an accurate model of each sample, the laser cut panel and the Serraglaze™. They are shown in Figure 6, and present geometrical and material properties as close as possible to the physical elements (see section 2.3.1 and 2.3.3).

Practically, in order to have only one tracing session (and not six), all the six screen positions were simulated at once by the way of six virtual screens. To avoid inter-reflections between the different detection surfaces, they were defined as perfect absorbers.

The rays were emitted from an annular grid, composed of 45 rings and sending about 6000 rays at wavelength 555 nm. The flux threshold (fractional value of starting flux for which a ray will be terminated) was set to 0.05. It was checked that a three times larger number of rays or a 50 times lower cut-off value did not significantly affect the results (variations lower than 1%).

FHG-IBP

The FHG-IBP Numerical Goniophotometer has been developed as an alternative method of including CFS into the process of daylight design and simulation [28, 30]. It represents an automated environment allowing to:

- configure the virtual test set up,
- to parameterize and combine CFS samples,
- and to post-process data for further use in daylight simulation.

The environment is based on the commercial forward ray tracing tool OptiCad™ [31] and generally follows the flux based method described earlier. The procedure has been validated against analytical and measured reference cases.

Generators for different kinds of CFS (like prismatic elements, laser cut panels, venetian blinds with different geometries and coatings and gratings)

[1] Lambda Research Corporation.

are provided. Individual façade components can be configured in a layer structure into compound systems.

The configuration of the virtual test set up, the specification of component parameters and the post processing functionality are integrated into a graphical user interface [30].

3.3 BTDF datasets and related error sources

The BTDF of both, a Serraglaze™ sample and the Laser Cut Panel were determined experimentally (measured) with the bidirectional video-goniophotometer and computationally (calculated) with both numerical goniophotometers. The samples have been numerically modelled according to the manufacturer's specifications. The model for the Serraglaze™ sample is depicted in Figure 6(b). For the Serraglaze™ sample however, it could not be clarified, if the physical sample and its numerical model were of the exact same type, as attempts to get exact manufacturer information failed.

While the BTDF datasets of both the Laser Cut Panel and the Serraglaze™ showed very close qualitative behaviours between measured and simulated values, significant deviations were found between them from a quantitative point of view. The hemispherical transmission values deduced from measurements were significantly lower than for both simulated datasets.

For the Laser Cut Panel, this can be explained by the strong impact of the thermal cutting of the panels on the light transmission features, which can result, especially for grazing incident angles, in strong differences with the ideal (modeled) system containing perfectly planar cuts. In addition it was found that the cuts in some panels were asymmetric (not truly perpendicular to the surface normal direction), which also results in asymmetric light transmission.

For the Serraglaze™, the bigger differences between measured and simulated are most likely to be found in the assumptions on geometry and material of the simulated sample. It could not be tracked whether technical changes had been introduced to the product, i.e. if the technical drawing on which the simulated sample was based on corresponded to the real sample. Also manufacturing inaccuracies are inevitable.

A systematical error in the simulation procedure is, however, very unlikely since other validation efforts for both applied numerical goniophotometers showed good performance [20, 21, 29, 32] In addition to this, the two pairs of simulated datasets for the Serraglaze™ and the Laser Cut Panel showed a close agreement, with average discrepancies of only 3,8 % for the hemispherical transmittance,

4. APPLIED SIMULATION METHODS

Two types of simulation approaches were tested: simulations using the samples' BTDF data and simulations based on ray-tracing only (Radiance based simulations). Below is presented a description of these methods in addition to a discussion about the potential related error sources.

4.1 Simulation methods using BTDF data

The common procedure for the BTDF based simulations is to combine the measured or calculated BTDF data with the outside luminance distribution to calculate a resulting flux distribution.

4.1.1 Equivalent luminaire method - ENTPE

The ENTPE method for CFS simulations is based on replacing the sample inner surface by an equivalent luminaire associated to an equivalent intensity distribution, which is obtained from the Photolux sky luminance map and the LESO-PB/EPFL measured BTDF data.

To create the equivalent intensity distribution, the 360,000 luminance values from Photolux were first reduced to 145 values representing the average luminance of the 145 zones (covering the whole hemisphere) at the incidence directions for which the BTDF data was measured.

For each of the 145 zones, resulting illuminance at the sample surface was calculated and multiplied by the BTDF value at each of the transmission directions of the BTDF data (every 5 degree in azimuth and zenith) to obtain the transmitted luminance in these directions.

For each transmission direction, the total transmitted luminance was obtained from the addition of the transmitted luminances from the 145 zones (at the incidence directions). This total luminance was then transformed into an intensity value that is equivalent to the combination of the sky and the material (in the given transmission direction).

The obtained intensity values in the different transmission directions were saved into an intensity distribution file using the standard IESNA format. This file was then used to conduct a lighting simulation within Lightscape 3.2, which was previously validated in artificial lighting calculations [25].

The simulations with an empty opening were conducted by using the intensity distribution files (1° resolution) produced by Photolux from the measured luminance maps.

4.1.2 CFS algorithm - FHG-IBP

The method is based on computing the intensity distribution on the internal surface of a façade element from BTDF data (measured or calculated) and the outside luminance distribution on the façade element [32]. It is independent of specific lighting simulation programs and generally can be incorporated into different standalone tools like complex fenestration system database and lighting simulation engines.

Since the BTDF data sets are being recorded for a restricted number of incident angles (generally the subdivision of the Hemisphere according to

Tregenza [33] is used) the data resolution on the incident side is normally significantly lower than the resolution on the emerging hemisphere. Implementing these raw data directly into superposition algorithms may result in artifacts and wrong predictions of the candle power distribution. Therefore, based on the geometric relations of the hemispherical subdivision scheme, a matched filter is used to pre-process the raw data in this CFS algorithm. This corresponds in general to a low-pass filtering of the data, i.e. reducing high frequent components and therefore attenuating “bumby” BTDF components in the final intensity distributions. The effect is illustrated in Figure 15.

Since the BTDF raw data sets are big in volume, data compression techniques are introduced and applied.

The procedure has so far been validated against selected analytical and data based test cases. A discussion of the limitations of the method can also be found in [32].

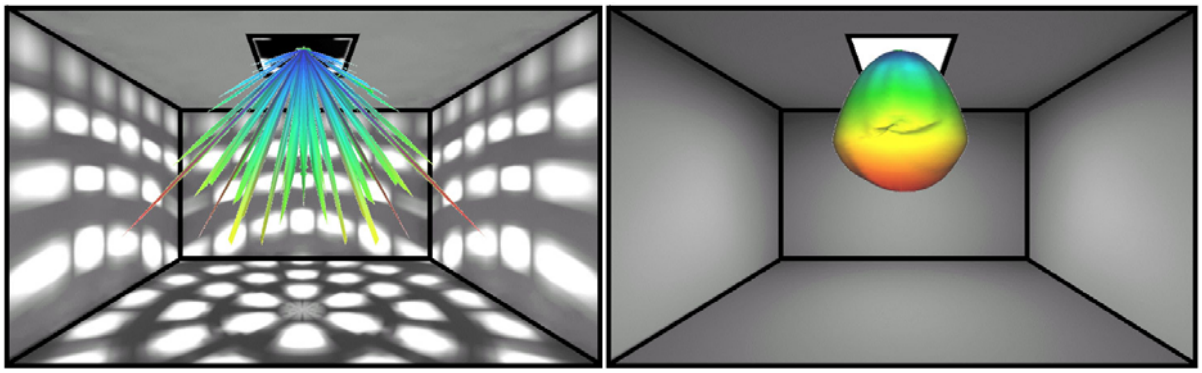

Figure 15. Influence of filter corrections. Left-hand figure: Superposition of the *unfiltered* indicatrices of diffusion. Right-hand figure: Superimposed *filtered* indicatrices of diffusion.

For this study an implementation of the method into to the RADIANCE program system was used. CFS were computed based on both measured (LESO) and simulated (IBP) BTDF datasets with an adapted RADIANCE version (which incorporates the method described above). All runs have been performed for the 5° sampled sky maps.

4.1.3 DElight

DElight is a general-purpose daylighting analysis tool that can calculate the illuminance on interior surfaces or control reference points from external natural light sources (typically the sky) that is transmitted through apertures into the space. Delight uses a radiosity-based method that calculates the direct and indirect light that illuminates each grid point of all the surfaces that define a space. Its features and use are further documented in [35, 36]. A DElight input was developed to match the specifications for the study scenarii. The procedure followed to obtain the results can be described as following:

The surface gridding resolution affects the accuracy of the results. The CFS aperture surface was gridded to 20x20, interior wall surfaces were gridded to 60x80, and the floor interior to 80x80. This particular gridding resolution is considered high-accuracy.

The LESO-PB/EPFL BTDFs were pre-processed into an internal DElight data representation, preserving the incident (Tregenza) directions and with a transmitted resolution based on 1250 equally distributed angular directions. Those pre-processed BTDFs were then used with the Radiance sky files (1°

resolution) in a sky-BTDF integration, to produce a directional luminance map of the light transmitted through the CFS in the aperture into the test box.

Internal surfaces were not defined for 3.6cm high edges of the finite-depth aperture. The actual aperture opening height was assumed to be 63.6cm above the floor for the empty opening and 64.3cm when the CFS was placed over the aperture. DElight instead uses an approximate “Reveal-depth” algorithm.

Because of the low (4.5%) internal surface reflectance, the inter-reflection calculations were limited to a “one-bounce” approximation.

4.2 Ray-tracing based model (Radiance)

This method is based on a calculation algorithm developed to model and simulate LCP in Radiance program system. The LCP transmits and reflects incident light rays, generating three possible emergent rays: the reflected, deflected and undeflected beams. For each ray incident upon an LCP, a linked function file calculates the fractions reflected, deflected and un-deflected, and the directions of these emergent beams. The developed algorithm is further detailed by Greenup et al. [37].

The LCP was modeled in Radiance using the *prism2* material primitive. This material primitive is used to simulate light redirection from prismatic glazings. It may be used to describe reflectance or transmittance, and allows for two ray redirections.

Following the material definition, a panel may be formed from the material using Radiance’s surface primitives. Only the planar surfaces polygon and ring may be used in conjunction with the prism2 material primitive.

Using this algorithm, it is possible to model any geometry involving the LCP with cuts normal to the panel surface. The model treats the LCP as a macroscopic entity of homogeneous light redirection properties, rather than a microscopic entity comprising several small air gaps. Multiple internal reflections and internal losses are considered. Two ray redirections are passed to the output, those being the most important of the three possible components.

The algorithm does not model non-flat cuts, and does not model cuts that are not normal to the surface of the panel. Thus, the proposed method was only applied to the LCP scenario of this paper and not to the Serraglaze^{TM} scenarii where the cuts are not normal to the surface of the sample.

LCP simulations were performed using Radiance (Desktop Radiance v2.0). Geometrical and material definitions were created to model the testing facility described above. The LCP material was modeled as planar surface with homogeneous light distribution characteristics, as described in above. The material has a refractive index of 1.49 and D/W ratio 0.66667 (thickness 6mm, cut spacing 4mm).

The sky was modeled with the measured sky luminance distribution provided at a 1° increment.

High quality simulation parameters were created, with ambient calculation parameters -ab 6 -aa .125 -ad 512 -as 256 -av 0 0 0. Illuminances were

predicted at the measurement points defined following the validation protocol described above, with the LCP in place and without any covering.

4.3 Error analyses

4.3.1 Errors with BTDF based methods

Similar approaches were applied in the three methods based on the use of BTDF raw data, and common error sources can be predicted in relation to the following points:

- Data interpolation at different levels: sky luminance map, BTDF output resolution, and calculated intensity or luminance distribution.
- BTDF-sky integration. The related error is mainly due to the difference in the resolutions of the BTDF input measurements and the sky luminance distribution. This usually leads to bumpy luminance maps (as shown in Figure 15) introducing errors to the simulation results. The IBP method applied a filtering procedure to solve this issue, which performs well for smooth (low frequent) sky luminance distributions independently of the type of BTDF (low frequent like diffuse glazing or high frequent i.e. with peaks like for LCP and Serraglaze). For high frequent sky distributions and BTDFs with high frequent components, the error in angular strong resolved domains of the final intensity distribution can increase [32].

Other error sources specific to each method can also be predicted like for example those related to the reveal-depth algorithm applied by DElight, or to the accuracy parameters defined in each of the tested methods.

4.3.2 Errors with Radiance LCP model

The Radiance lighting simulation tool has been subjected to numerous validation exercises [34, 38, 39, 40, 41]. Radiance simulations compared very well with measurement for both simple and complex geometries, providing errors generally less than 10%.

However, some additional error can be expected for this study, related to the simplified laser cut panel modeling algorithm. The extent of this additional error has been estimated to 5% through comparison of simulated and measured luminous transfer efficiencies [42].

5. COMPARISON BETWEEN SIMULATION RESULTS AND MEASUREMENTS

5.1 Serraglaze™ scenarii

Simulation results for the Serraglaze™ scenarii are illustrated in Figures 16 to 18 and referred to by the contributing party, as follows:

- DElight simulations: simulations performed at LBNL using DElight simulation tool based on LESO-PB/EPFL measured BTDF
- ENTPE simulations: Lightscape simulations performed at ENTPE employing the equivalent luminaire method based on LESO-PB/EPFL measured BTDF
- IBP simulations with measured BTDF: Simulations performed at FHG-IBP using RADIANCE – integrated CFS algorithm , applying BTDF measured at EPFL
- IBP simulations with calculated BTDF: Simulations performed at FHG-IBP using Radiance-integrated CFS algorithm, applying BTDF determined by IBP numerical goniophotometer

Bare opening results (see A1 and A2 of Figures 16 to 18): Good agreement with reference data was generally observed for the majority of simulation results that were either within the tolerance bounds or very close to the lower boundary. The exceptions were for DElight results at the upper wall point for scenarii 1, 2 and 3 (see A2 of Figures 16 to 18), and for the ENTPE results at the upper wall point for scenario 2 (see Figure 17(A2)) and at both the ground and wall points for scenario 3 (see Figures 18(A1) and 18(A2)). It also can be noted that the agreement is better in scenario 1 than in the two other scenarii, and that scenario 3 shows the least agreement.

Serraglaze results (see B1 and B2 of Figures 16 to 18): Good agreement with reference data is generally observed for DElight and IBP-Measured BTDF results, but not for the IBP-Calculated BTDF and ENTPE results. Same as for the bare opening, DElight results showed less agreement at the wall points and generally the agreement decreased between scenarii 1 to 3 for all methods.

Hemi-Directional Transmittance (HDT) results (see C1 and C2 of Figures 16 to 18): Observations were similar to those made for the Serraglaze results with a slightly lower agreement. In addition, it was noted a very bad agreement for all methods at wall points in scenaii 2 and 3 (see Figure 17(C2) and 18(C2)).

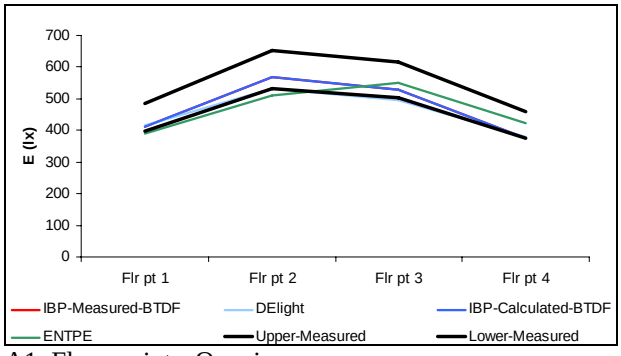

A1: Floor points, Opening

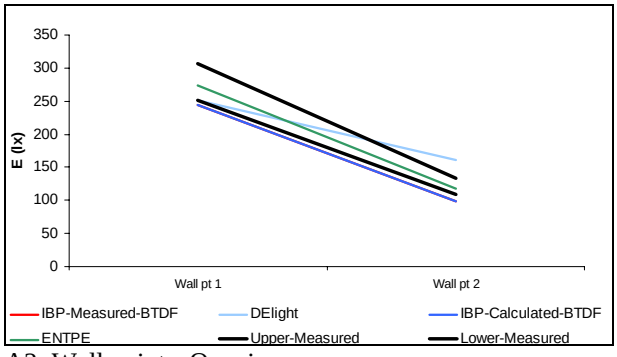

A2: Wall points, Opening

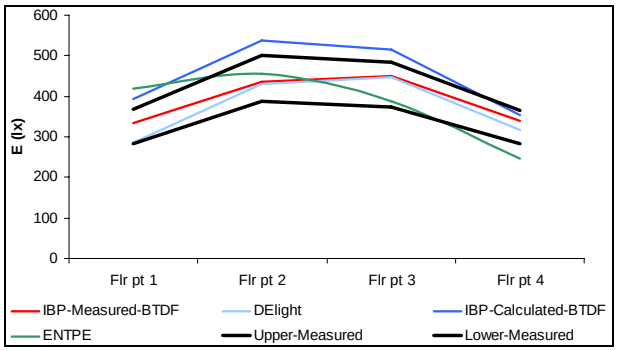

B1: Floor points, Serraglaze

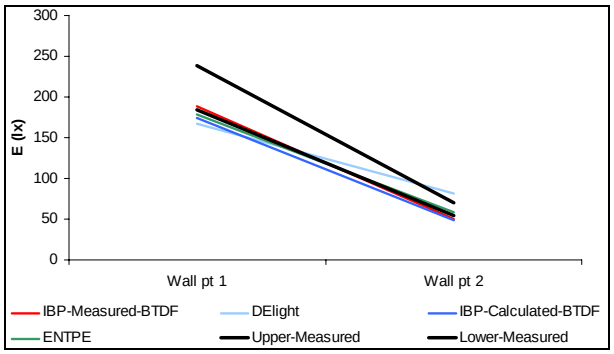

B2: Wall points, Serraglaze

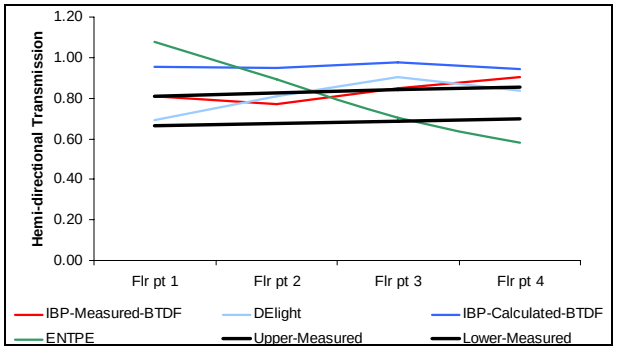

C1: Floor points, HDT

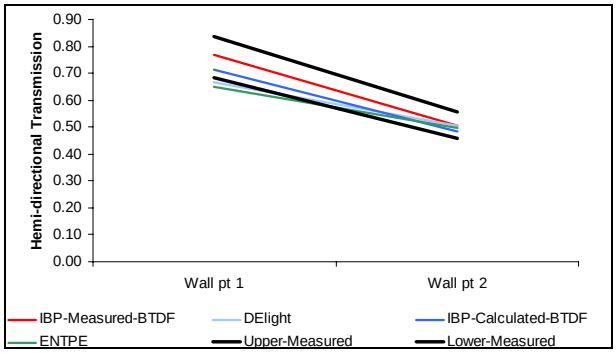

C2: Wall points, HDT

Figure 16. Scenario 1 results

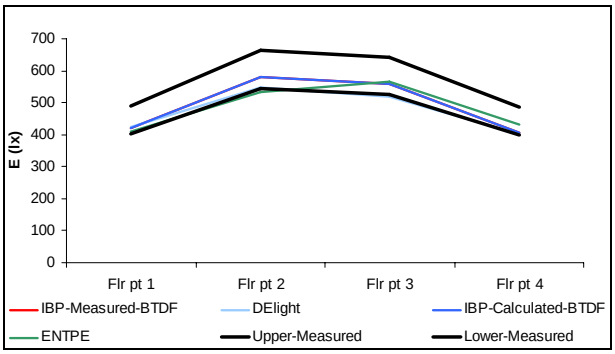

A1: Floor points, Opening

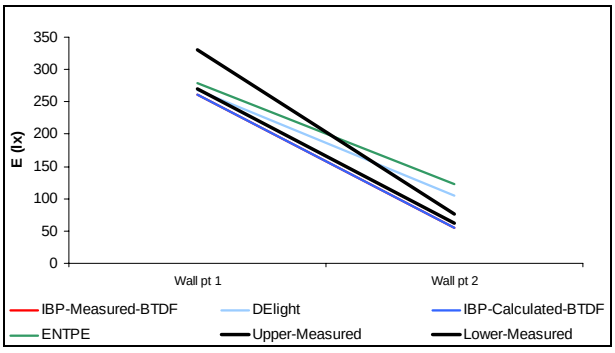

A2: Wall points, Opening

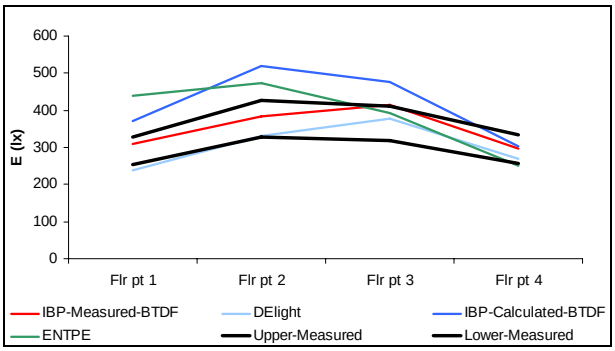

B1: Floor points, Serraglaze

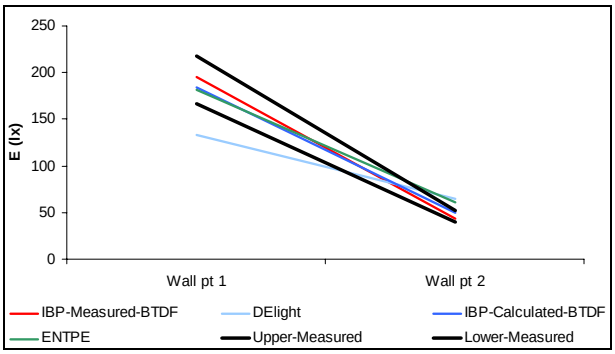

B2: Wall points, Serraglaze

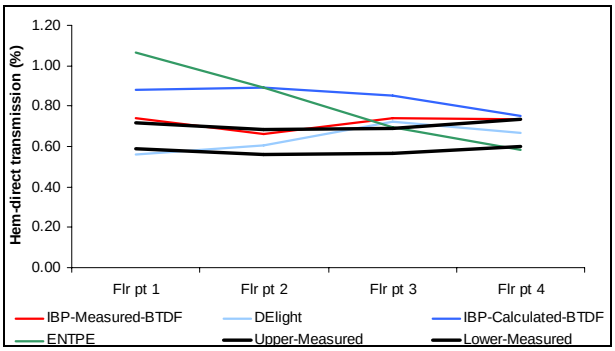

C1: Floor points, HDT

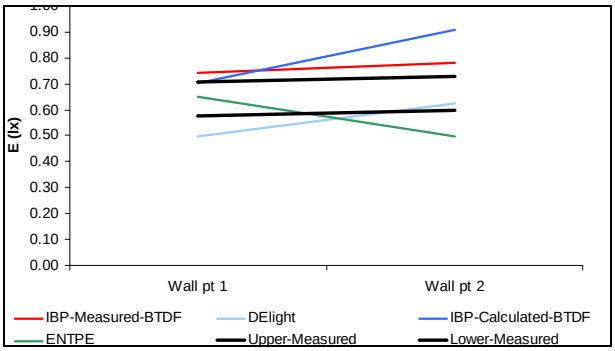

C2: Wall points, HDT

Figure 17. Scenario 2 results

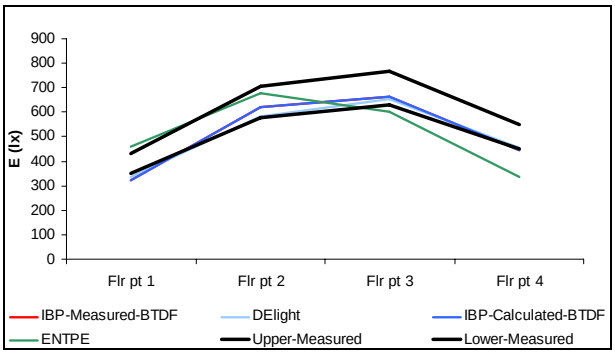

A1: Floor points, Opening

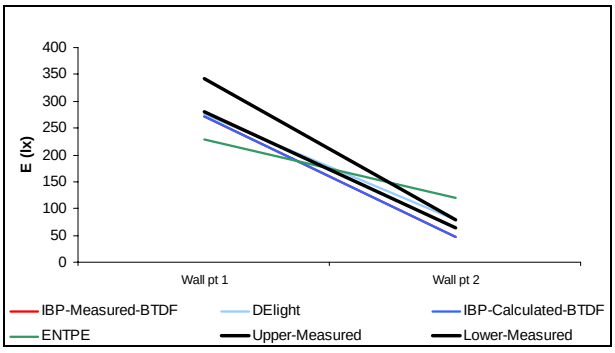

A2: Wall points, Opening

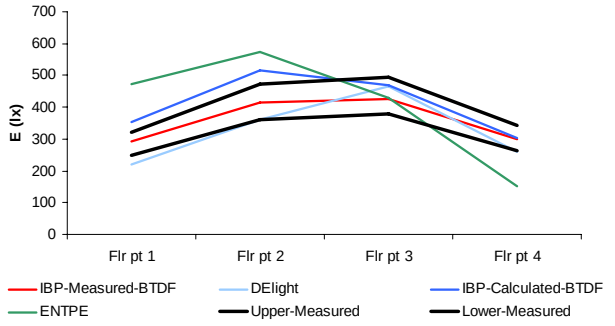

B1: Floor points, Serraglaze

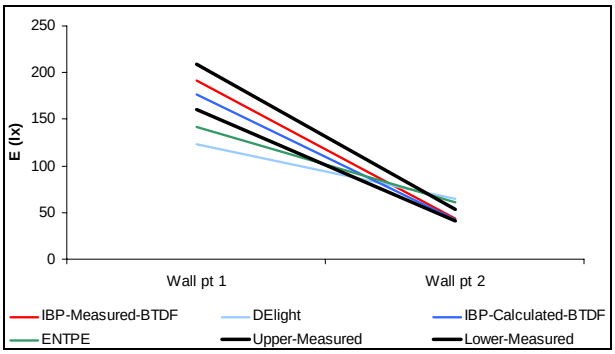

B2: Wall points, Serraglaze

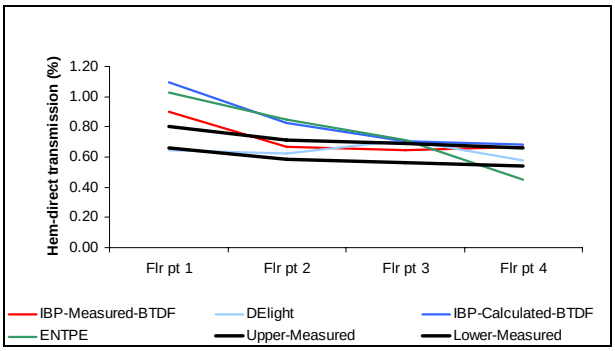

C1: Floor points, HDT

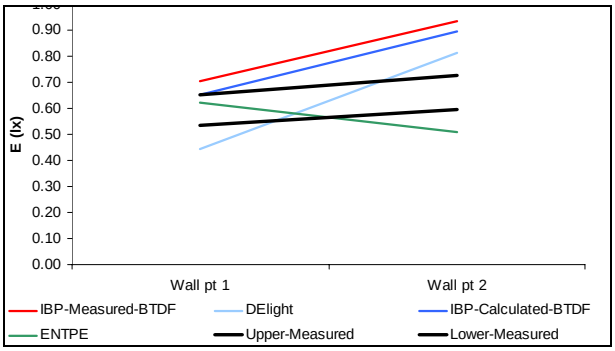

C2: Wall points, HDT

Figure 18. Scenario 3 results

5.2 LCP Scenario

Simulation results for the LCP scenario are illustrated in Figure 19 and referred to by the contributing party, as follows:

- DElight simulations: simulations performed at LBNL using DElight simulation tool based on LESO-PB/EPFL measured BTDF
- ENTPE simulations: Lightscape simulations performed at ENTPE employing the equivalent luminaire method based on LESO-PB/EPFL measured BTDF
- IBP simulations: Simulations performed at FHG-IBP using Radiance-integrated CFS algorithm, applying BTDF measured at EPFL
- Radiance simulations: Radiance LCP simulations employing analytical LCP modeling algorithm

The reference data of the LCP scenario was particularly interesting by highlighting the bi-directional effect of the CFS thanks to the directionality of the sky luminance map. Figure 20 shows the effect of the LCP where it enhanced the uniformity of the illuminance on the floor.

Bare opening results (see Figures 19(A1) and 19(A2)): Good agreement with reference data was generally observed for the majority of simulation results where only the predictions provided by the IBP and Radiance algorithms extended outside of the tolerance bounds. The highest disagreement was observed at the wall upper point for IBP simulation.

LCP results (see Figures 19(B1) and 19(B2)): All methods gave results within the tolerance bounds except for ENTPE simulation where illuminance values were under-predicted at floor points 6 and 7 (see Figure 19(B1).

HDT results (see Figures 19(C1) and 19(C2)): Observations were similar to those made for the LCP results except for the IBP results at the wall upper point (See Figure 19(C2), which reflects the disagreement observed at this point for the IBP opening results (See Figure 19(A2)).

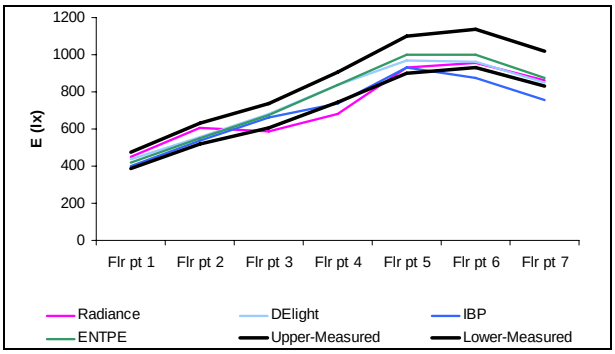

A1: Floor points, Opening

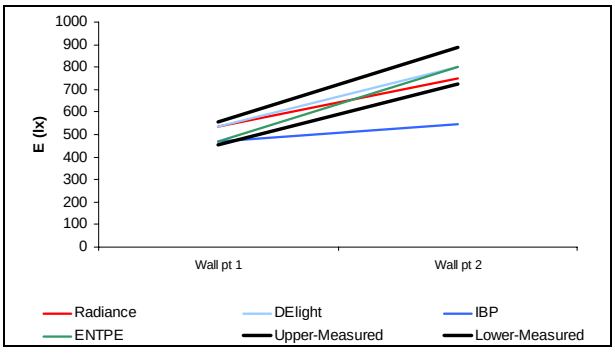

A2: Wall points, Opening

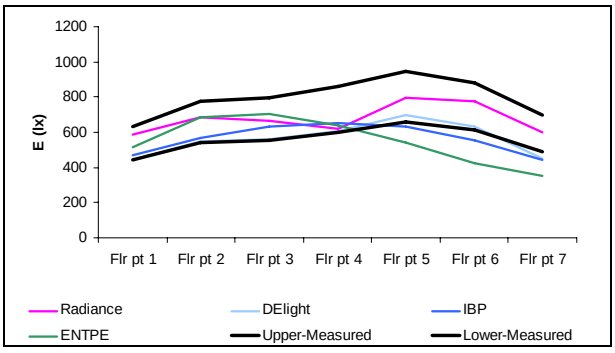

B1: Floor points, LCP

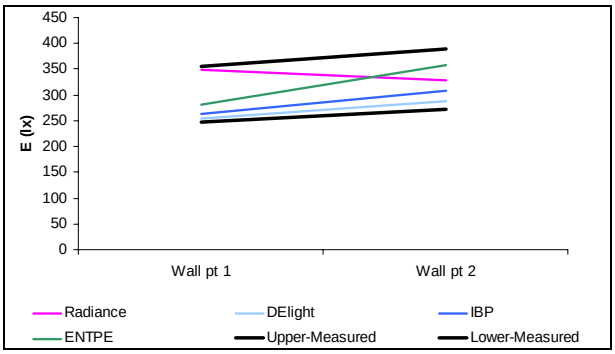

B2: Wall points, LCP

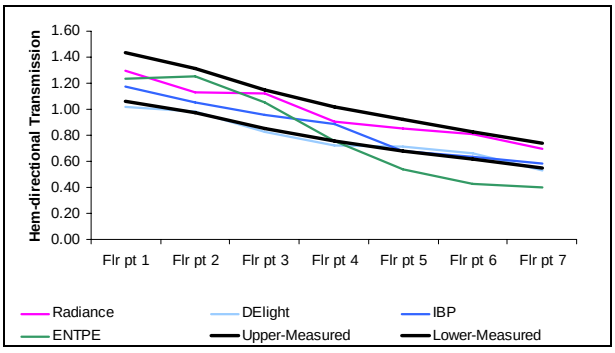

C1: Floor points, HDT

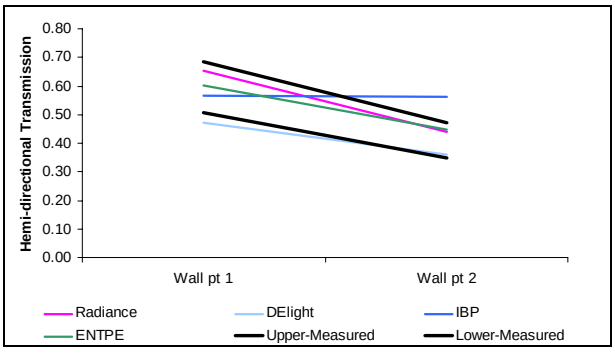

C2: Wall points, HDT

Figure 19. LCP Scenario results

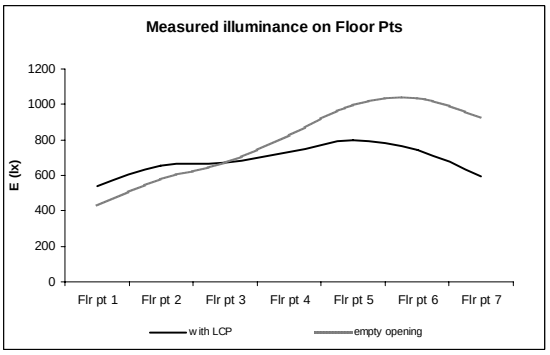

Figure 20. Influence of LCP on the illuminance distribution inside the scale model

5.3 Results analyses

Based on the results and the observations presented above, the following points could be highlighted:

- The decrease in agreement (between simulation results and reference data) observed for Serraglaze scenarii 1 to 3 can be attributed to the near field error source which is more present in scenario 3 (see to section 2.4.1).
- The decrease in agreement between IBP-Measured BTDF and IBP-Calculated BTDF for the Serraglaze scenarii can be attributed to the difference in the BTDF raw data. It can be supposed that this difference is mainly related to the accuracy in the description of the sample knowing that this description could not be confirmed by the manufacturer.
- DElight disagreement at the upper wall point for the Serraglaze scenarii can be attributed to the approximations of the window reveal-depth algorithm.
- ENTPE disagreement for LCP results (with the sample) can be attributed to the bumpiness of the calculated intensity distribution as discussed in sections 4.1.2 and 4.3. Figure 21(b) shows the bumpy effect on the illuminance distribution for ENTPE results. However, despite this disagreement, the ENTPE method was capable of predicting the bi-directional effect of the LCP (although with a slight exaggeration): the Figure 21 shows that the bright spot on the North wall of the empty opening results (a), was correctly redirected to the South wall in the LCP results (b).

(a) 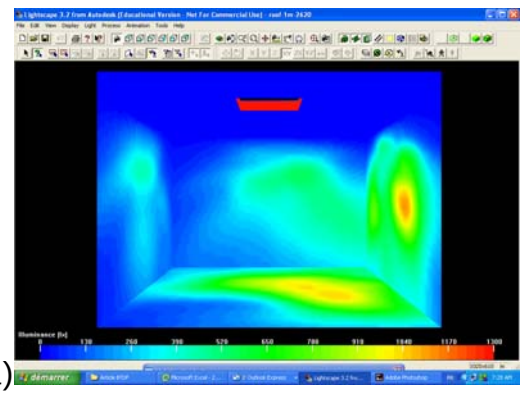 (b) 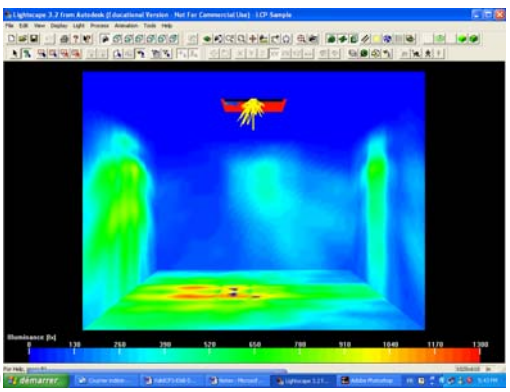

Figure 21. Illuminance distribution obtained by ENTPE method for LCP scenario. (a) shows results with bare opening while (b) shows results with the LCP sample.

6. CONCLUSIONS

The applied validation approach showed to be useful in assessing the capabilities of the tested simulation methods in predicting the performance of CFS under given sky conditions. The simplicity of the test cases allowed to identify the weakness areas of the simulation methods.

The results of this study proved the capability of the tested methods to quantitatively simulate CFS light distribution effects in the room: Overall, the comparison of reference data and simulations showed quite satisfactory results. A few difficulties were identified. However, given the quite complex CFS materials and simulation algorithms involved, these results are encouraging. The level of accuracy achieved in this study should be acceptable for design studies.

This work also showed the importance of the accuracy in describing the CFS for ray-tracing simulations or for methods using calculated BTDF. The resolution of the measured or calculated BTDFs showed to be an important tissue too.

Finally some recommendations could be concluded from this study:

- For future validation data, it would be useful to measure and use internal luminance maps as reference data.
- The use of higher resolutions in assessing BTDF should be considered to avoid related error sources, specially that existing numerical assessment methods allow reducing time and cost constraints. The validation approach applied in this study can be used to define an optimized resolution through parametric studies.
- The use of BTDF based simulation methods should be optimised through developing a wide BTDF database for existing CFS.

7. REFERENCES

[1] Ballinger, J. and Lyons, P. (1998). Advanced glazing and associated materials for solar and building applications. Report for IEA SHC Task 18, Draft Final Report for Subtask A.

[2] International Energy Agency (2000). Daylight in Buildings - A source book on daylighting systems and components. IEA SHC Task 21 / ECBCS Annex 29, Berkeley.

Kischkoweit-Lopin, M. (2002). An overview of daylighting systems. Solar Energy, 73(2):7782.

[3] Mitanchey, R., Periole, G., and Fontoynont, M. (1995). Goniophotometric measurements: Numerical simulation for research and development applications. Lighting Research and Technology, 27(4):189–196.

[4] Scartezzini, J.-L., Compagnon, R.,Ward, G., and Paule, B. (1994). Computer daylighting simulation tools. Technical report, University of Geneva / EPFL, Lausanne.

[5] Reinhart, C. and Herkel, S. (2000). The simulation of annual daylight illuminance distributions a state-of-the-art comparison of six RADIANCE-based methods. Energy and Buildings, 32(2):167–187.

[6] Roy, G. (2000). A comparative study of lighting simulation packages suitable for use in architectural design. Technical report, Murdoch University, Perth, Western Australia.

[8] Mitchell, R., Kohler, C., Arasteh, D., Carmody, J., Huizenga, C., and Curcija, D. (2003). THERM 5 / WINDOW5 NFRC Simulation Manual. Window & therm documentation, Lawrence Berkeley National Laboratory, Berkeley, CA.

[9] Illuminating Engineering Society of North America (1993). Lighting Handbook. IESNA, New York.

[10] Schweizerische Lichttechnische Gesellschaft (1992). Handbuch f¨ur Beleuchtung. Ecomed Verlag, Landsberg.

[11] Commission Internationale de l'Eclairage (1996). The photometry and goniophotometry of luminaires. CIE, 121.

[12] Commission Internationale de l'Eclairage (1977). Radiometric and photometric characteristics of materials and their measurement. CIE, 38(TC-2.3).

[13] Papamichael, K., Klems, J., and Selkowitz, S. (1988). Determination and Application of Bidirectional Solar-Optical Properties of Fenestration Materials. Technical Report LBL-25124, Lawrence Berkeley National Laboratory, Berkeley.

[14] Apian-Bennewitz, P. (1994). Designing an apparatus for measuring bidirectional reflection/ transmission. In Proceedings SPIE Vol. 2255, Optical Materials Technology for Energy Efficiency and Solar Energy Conversion XIII, pages 697–706.

[15] Bakker, L. and van Dijk, D. (1995). Measuring and processing optical transmission distribution functions of TI-materials. Private Communication, TNO Building and Construction Research, Delft.

[16] Breitenbach, J. and Rosenfeld, J. (1998). Design of a Photogoniometer to Measure Angular Dependent Optical Properties. In Proceedings of International Conference on Renewable Energy Technologies in Cold Climates, pages 386–391, Ottawa, Canada. Solar Energy Society of Canada Inc.

[17] Andersen, M., Michel, L., Roecker, C., and Scartezzini, J.-L. (2001). Experimental assessment of bi-directional transmission distribution functions using digital imaging techniques. Energy and Buildings, 33(5):417–431.

[18] Mitanchey, R., Escaffre, L., and Marty, C. (2002). From optical performances characterization of a redirecting daylight material to daylighting simulations. In Proceedings of the 3rd European Conference on Energy Performance & Indoor Climate in Buildings EPIC 2002, pages 721–726, Lyon, France, Oct. 23-26. ENTPE.

[19] De Boer, J. (2003). Encorporation of numerical goniophotometry into daylighting design. In Proceedings CISBAT 2003, pages 229–234, Lausanne, Oct. 8-9. EPFL.

[20] Andersen, M., Rubin, M., and Scartezzini, J.-L. (2003). Comparison between ray-tracing simulations and bi-directional transmission measurements on prismatic glazing. Solar Energy, 74(2):157–173.

[21] Andersen, M., Rubin, M., Powles, R., Scartezzini, J.-L. (2005). Bi-directional transmission properties of venetian blinds: experimental assessment compared to ray-tracing calculations, Solar Energy, 78(2):187-198.

[22] Maamari, F., Fontoynont, M. (2002). Use of IEA-SHC Task 21 C benchmarks to assess performance of Lightscape 3.2 in daylighting calculations. In: Lyon, France, Proceedings of EPIC conference, pp. 709-714.

[23] Commission Internationale de l'Eclairage (2004). Test cases to assess the accuracy of Lighting computer programs, Under review.

[24] Slater, A., Graves, H. (2002). Benchmarking Lighting Design Software. TM 28/00. London: CIBSE, 2002, 33 p.

[25] Maamari, F. (2004). Simulation numérique de l'éclairage, limites et potentialités. PhD in Civil Engineering. INSA de Lyon, Lyon, 280 p.

[26] Coutelier B., Dumortier D. (2003). Luminance calibration of the Nikon Coolpix 990 digital camera. In Proceedings of the 25th Session of the CIE, San Diego, 2003, Vol. 1, D3-56.

[27] Mardaljevic, J. Quantification of Parallax Errors in Sky Simulator Domes for Clear Sky Conditions Lighting Res. Technol. 34(4) 2002, pp 313-332

[28] Andersen M.; de Boer J.: Goniophotometry and assessment of bidirectional photometric properties of complex fenestration systems. Energy and Buildings, Under review.

|29] Andersen, M. (2004). Innovative bidirectional video-goniophotometer for advanced fenestration systems. PhD thesis, EPFL, Lausanne.

[30] de Boer, J. : Numerical Goniophotometer. User Manual, Fraunhofer Institute for Building Physics, Stuttgart (2004).

[31] OptiCad: Opticad, Optical Analysis Program User's Guide Version 7.0. Opticad Corporation, Santa Fe (2001).

[32] de Boer, J,: Modelling indoor illumination by complex fenestration systems using bidirectional photometric data. Energy and Buildings, under review (2004).

[33] Tregenza, P.: Subdivision of the sky hemisphere for luminance measurements, Lighting Research and Technology 19, Nottingham (1987), H.1, pp. 13-14.

[34] Fontoynont, M., P. Laforgue, R. Mitanchey, M.E. Aizlewood, J. Butt, W. Carroll, R. Hitchcock, H. Erhorn, J. De Boer, L. Michel, B. Paule, J.-L. Scartezzini, M. Bodart and G.G. Roy, 1999. Validation of Daylighting Simulation Programs. November. Vaulx-en-Velin, France: International Energy Agency Solar Heating and Cooling Task 21 / Energy Conservation in Buildings and Community Systems Programme Annex 29.

[35] Hitchcock, R.J., Carroll, W. L. (2003). DElight: A Daylighting and Electric Lighting Simulation engine, International Building Performance Simulation Association, IBPSA BS 2003, Eindhoven, Netherlands.

[36] U. S. Department of Energy, (September 2004),EnergyPlus Engineering Document.
http://www.eere.energy.gov/buildings/energyplus/pdfs/engineeringdoc.pdf

[37] Greenup, P., Edmonds, I.R. and Compagnon, R. (2000), RADIANCE algorithm to simulate laser-cut panel light-redirecting elements, Lighting Res. Technol., 32(2), 49-54.

[38] Mardaljevic, J., 1995. Validation of a Lighting Simulation Program under Real Sky Conditions. Lighting Res. Technol., 27 (4), 181-188.

[39] Mardaljevic, J., 2000. Daylight Simulation: Validation, Sky Models and Daylight Coefficients. Leicester, UK: De Montfort University.

[40] Mardaljevic, J., 2001. The BRE-IDMP Dataset: A New Benchmark for the Validation of Illuminance Prediction Techniques. Lighting Res. Technol., 33 (2), 117-136.

[41]Khodulev, A.B. and E.A. Kopylov, 1996. Physically Accurate Lighting Simulation in Computer Graphics Software (World Wide Web site). url: rmp.kiam.ru/articles/pals, accessed: 22 Jan.

[42] Greenup, P.J. (2004), Development of Novel Technologies for Improved Natural Illumination of High Rise Office Buildings, PhD Thesis, Queensland University of Technology, Brisbane.

8. LIST OF CONTACT PERSONS

TO BE UPDATED

Task 31 Operating Agent:

Nancy Ruck
University of Sydney
Dept. of Architecture & Design Science
Sydney NSW 2006, Australia
Phone: +61 2 9351 4029
Fax: +61-2-9351-3031

Leader Subtask A:

Leader Subtask B:

Leader Subtask C:

Hans Erhorn
Fraunhofer Institute for Building Physics
Nobelstraße 12
D - 70569 Stuttgart, Germany
Fax: +49-711-970-3399

Members of Subtask C:

Australia:

Belgium:

Canada:

Denmark:

France:

Germany:

Sweden:

Switzerland:

United States:

9. IEA INFORMATION

OVERVIEW OF THE IEA AND THE SOLAR HEATING AND COOLING AGREEMENT

INTERNATIONAL ENERGY AGENCY

The International Energy Agency, founded in November 1974, is an autonomous body within the framework of the Organization for Economic Cooperation and Development (OECD) which carries out a comprehensive program of energy cooperation among its 24 member countries. The European Commission also participates in the work of the Agency.

The policy goals of the IEA include diversity, efficiency and flexibility within the energy sector, the ability to respond promptly and flexibly to energy emergencies, the environmentally sustainable provision and use of energy, more environmentally-acceptable energy sources, improved energy efficiency, research, development and market deployment of new and improved energy technologies, and cooperation among all energy market participants.

These goals are addressed in part through a program of international collaboration in the research, development and demonstration of new energy technologies under the framework of 40 Implementing Agreements. The IEA's R&D activities are headed by the Committee on Energy Research and Technology (CERT) which is supported by a small Secretariat staff in Paris. In addition, four Working Parties (in Conservation, Fossil Fuels, Renewable Energy and Fusion) are charged with monitoring the various collaborative agreements, identifying new areas for cooperation and advising the CERT on policy matters.

IEA SOLAR HEATING AND COOLING PROGRAM

The Solar Heating and Cooling Program was one of the first collaborative R&D agreements to be established within the IEA, and, since 1977, its Participants have been conducting a variety of joint projects in active solar, passive solar and photovoltaic technologies, primarily for building applications. The nineteen members are:

Australia	Japan
Austria	Mexico
Belgium	The Netherlands
Canada	New Zealand
Denmark	Norway
European Commission	Spain
Finland	Sweden
France	Switzerland
Germany	United Kingdom
Italy	United States

A total of 26 projects or "Tasks" have been undertaken since the beginning of the Solar Heating and Cooling Program. The overall program is monitored by an Executive Committee consisting of one representative from each of the member countries. The leadership and management of the individual Tasks are the responsibility of Operating Agents.

These Tasks and their respective Operating Agents are:

*Task 1: Investigation of the Performance of Solar Heating and Cooling Systems - Denmark
*Task 2: Coordination of Research and Development on Solar Heating and Cooling - Japan
*Task 3: Performance Testing of Solar Collectors - Germany/United Kingdom
*Task 4: Development of an Insulation Handbook and Instrument Package - United States
*Task 5: Use of Existing Meteorological Information for Solar Energy Application - Sweden
*Task 6: Solar Systems Using Evacuated Collectors - United States
*Task 7: Central Solar Heating Plants with Seasonal Storage - Sweden
*Task 8: Passive and Hybrid Solar Low Energy Buildings - United States
*Task 9: Solar Radiation and Pyranometry Studies - Canada/Germany
*Task 10: Solar Material Research and Testing - Japan
*Task 11: Passive and Hybrid Solar Commercial Buildings - Switzerland
*Task 12: Building Energy Analysis and Design Tools for Solar Applications - United States
*Task 13: Advanced Solar Low Energy Buildings - Norway

*Task 14: Advanced Active Solar Systems - Canada
Task 15: Not initiated
*Task 16: Photovoltaics in Buildings - Germany
*Task 17: Measuring and Modelling Spectral Radiation - Germany
*Task 18: Advanced Glazing Materials - United Kingdom

*Task 19: Solar Air Systems - Switzerland
*Task 20: Solar Energy in Building Renovation - Sweden
Task 21: Daylighting in Buildings - Denmark
Task 22: Building Energy Analysis Tools - United States
Task 23: Optimization of Solar Energy Use in large Buildings - Norway
Task 24: Solar Procurement - Sweden
Task 25: Solar Assisted Cooling Systems for Air Conditioning of Buildings (Task Definition Phase)
Task 26: Solar Combisystems – Austria
Task 27: Performance of Solar Façade Components
Task 28: Sustainable Solar Housing
Task 29: Solar Crop Drying
TASK 31 Daylighting Buildings in the 21st Century - Australia
TASK 32 Advanced Storage Concepts for Solar Thermal Systems in Low Energy Buildings
TASK 33 Solar Heat for Industrial Process
TASK 34 Testing and Validation of Building Energy Simulation Tools

**Completed*